ELSEVIER

Journal of Molecular Catalysis A: Chemical 185 (2002) 223–235

JOURNAL OF MOLECULAR CATALYSIS A: CHEMICAL

www.elsevier.com/locate/molcata

Characterization of MAO-modified silicas

Daniela Bianchini [a], João Henrique Zimnoch dos Santos [a,*], Toshiya Uozumi [b], Tsuneji Sano [b]

[a] *Departamento de Química Inorgânica, Instituto de Química, Universidade Federal do Rio Grande do Sul, Av. Bento Gonçalves 9500, Porto Alegre, RS 91509-900, Brazil*

[b] *School of Materials Science, Japan Advanced Institute of Science and Technology,1-1 Asahidai, Tatsunokuchi, Ishikawa 923-1292, Japan*

Received 29 October 2001; received in revised form 3 January 2002; accepted 29 January 2002

Abstract

A series of methylaluminoxane (MAO)-modified silicas were prepared by the impregnation method, using MAO toluene solution with concentration ranging from 0.0 to 20.0 wt.% Al/SiO_2. The resulting solids were characterized by complementary spectroscopic and volumetric techniques, namely, inductively-coupled plasma-optical emission spectroscopy (ICP-OES), ultraviolet–visible spectroscopy (UV–VIS), X-ray photoelectron spectroscopy (XPS), diffuse-reflectance (DRIFTS) infrared spectroscopy, scanning electron microscopy (SEM) analysis and electron probe microanalysis (EPMA). Resulting texture of the modified silicas were analyzed by nitrogen sorption based on the Brunauer–Emmett–Teller (BET) method. Surface saturation seems to take place at about 10 wt.% Al/SiO_2, based on the consumption of silanol groups, which were monitored by DRIFTS. XPS Al 2p spectra indicate the generation of two surface species for Aluminum content higher than 10 wt.% Al/SiO_2. Considering the presence of trimethylaluminum (TMA) in commercial MAO, it is very likely that depending upon the Al concentration, a competitive reaction for the immobilization sites (silanol groups) might take place, specially due to the higher reactivity and less steric effect played by TMA, therefore, generating different Al species.

Keywords: Silica; MAO; TMA; XPS; DRIFTS

1. Introduction

Metallocene catalysts, activated by methylaluminoxane (MAO), are recognized by their high activity, production of polymers with a narrow molecular weight distribution and homogeneous comonomer distribution in the polymeric chain [1]. Highly active soluble metallocene catalysts can be used as drop in substitute in existing solution and high pressure manufacturing plants. For gas-phase and slurry processes, however, such catalysts have to be immobilized, usually by supporting on appropriate carrier, while retaining the essential characteristics of their homogeneous analogs.

Many approaches for supporting metallocenes have been reported in the literature [2], including direct immobilization, functionalization of silica or preparation of hybrid sol–gels [3]. Methods based on the silica chemical treatment with MAO or trimethylaluminum (TMA) prior to metallocene immobilization are believed to generate more active supported catalysts (in comparison with direct grafting). In such systems, it has been proposed that metallocene complexes be bonded to the support by loosely ionic interaction [4].

* Corresponding author.
E-mail address: jhzds@iq.ufrgs.br (J.H.Z. dos Santos).

1381-1169/02/$ – see front matter
PII: S1381-1169(02)00047-X

The role of MAO is not completely elucidated. MAO alkylates, the metallocene catalyst generating coordinatively unsaturated cationic species by substitution of one chlorine atom by an alkyl group and extraction of the second chlorine atom. There are evidences that this type of compounds comprise the catalytic active species for olefin polymerization. MAO works as a counterion, keeping the catalytic species in a cationic state and playing the role of a non-coordinating anion. Trialkylaluminum (AlR_3) may work in the same way, but the resulting anion too strongly coordinates to the metallocene cation, making the active site not available enough for the olefin insertion. Other functions have been attributed to MAO including the stabilization of the active species (counterion), prevention of bimolecular deactivation and water and oxygen milieu scavenger [5].

The structure of MAO is also not completely elucidated. Barron [6] was the first who obtained aluminoxanes in crystalline state and structurally characterized some alkylaluminoxane $[(R_2Al)_2O]_n$ and $(RAlO)_n$, containing *t*-Bu groups. Nevertheless, the structure of aluminoxanes with other alkyl groups, especially with methyl and ethyl ones, are still to be solved [7]. Each of the building blocks of aluminoxanes contains two or three acidic or basic centers, which are responsible for the reactions leading to oligomer formation, reaction with electron donors. Such properties render the preparation of aluminoxane in crystalline form and their crystal structure determination is difficult. Moreover, the direct elucidation of the structure and of the function of MAO is hindered by the presence of multiple equilibra such as disproportionation reactions between oligomeric chains. For the sake of simplicity MAO has been usually represented as having linear chain or cyclic ring structures $[Al(Me)–O–]_n$ containing three-coordinate aluminum centers.

Commercial MAO is the product of TMA partial hydrolysis and includes the oligomeric molecules of MAO, and usually a significant amount of TMA associated with MAO [8]. Inspite of an equilibrium between both species has been usually proposed, recently, based on FT-IR spectroscopy monitoring, Eilertsen et al. [9] observed no reaction between TMA and MAO in toluene solution. Monitoring by DRIFTS and mass-spectrometric methods has evidenced that solid MAO releases TMA under heating between 293 and 523 K [10].

In a previous work, we determined the adsorption isotherms of MAO and TMA for different commercial silicas [11]. In the present work, we report the characterization of MAO-supported silicas containing Al amount below and above the saturation level (∼8–10 wt.% Al/SiO_2). Aluminum content were determined by inductively-coupled plasma-optical emission spectroscopy (ICP-OES). Surface species were characterized by complementary spectroscopic techniques, namely, ultraviolet–visible spectroscopy (UV–VIS), transmission (FT-IR) infrared spectroscopy, X-ray photoelectron spectroscopy (XPS), diffuse-reflectance (DRIFTS) infrared spectroscopy. Resulting texture of the modified silicas were analyzed by nitrogen sorption based on the Brunauer–Emmett–Teller (BET) method. Particle shape image and X-ray maps of the catalyst elements were obtained through scanning electron microscopy (SEM) analysis and electron probe microanalysis (EPMA).

2. Experimental

2.1. Materials (chemicals)

Silica Grace 948 was activated under vacuum ($<10^{-4}$ mbar) for 16 h at 723 K. The support was then cooled to room temperature under dynamic vacuum and stored under dried argon. MAO (supplied by Witco, 10.0 wt.% toluene solution, 1.7 Al as TMA, average molar mass 900 g mol^{-1}) and MAO-modified silica (Witco), having 24.4 wt.% Al/SiO_2 were manipulated as received. Pura grade toluene was deoxygenated and dried by standard techniques.

2.2. Preparation of modified silicas

All impregnation experiments were performed under inert atmosphere using the Schlenk technique. Typically, 1.0 g of preactivated silica was impregnated with MAO toluene solutions at 298 K, corresponding to metal contents comprised between 0.0 and 20.0 wt.% Al/SiO_2. The solvent was removed by vacuum.

The Al content was measured by ICP-OES in a Seiko equipment (SPS 7700). The samples were previously attacked by acid digestion using H_2SO_4 2N solution.

XPS were taken with an Alvac PHI 5600 Esca System (Physical Electronics), monochromated Al Kα radiation (1486.6 eV). Acquisition was carried out at room temperature in high-resolution mode (0.1 eV step, 23.5 eV pass energy) for the Al 2p and Si 2p regions. The samples were mounted as thin films on an adhesive copper tape in a glove box, introduced into a transfer chamber and then evacuated to 10^{-6} Torr in 90 min using a turbomolecular pump. During data collection, an ion-getter pump kept the pressure in the analysis chamber under 10^{-9} Torr. Takeoff angles (angle between the surface plane and the irradiator) of 20, 45, 60 and 75° were used to control the sampling depth in the XPS experiment. For each of the XPS spectra reported, an attempt has been made to deconvolute the experimental curve in a series of peaks representing photoelectron emission from atoms in different chemical environments. These peaks are described as a mixture of Gaussian and Lorentzian contributions to take instrumental error into account together with the characteristic shape of photoemission peaks. All binding energy values were charge referenced to the Si 2p at 103.3 eV.

UV–VIS analysis was performed in a DW-2000 spectrometer (Sim-Aminco, USA) equipped with a beam scrambler, which diffuses the entering light to form a uniform field of illumination, eliminating any spatial differences between beams. In order to increase the sample transparency and the viscosity, the solids were mixed with Nujol to form a slurry. All the samples were prepared in a glove box in quartz cells (1.0 cm pathlength). The absorption spectra were recorded under dry N_2 between 250 and 550 nm, having Nujol as reference.

A commercial diffuse-reflectance accessory with thermal control was employed for DRIFTS measurements in a JIR-7000 Jeol Spectrometer. The samples were transferred under N_2 atmosphere and evacuated before, during, and between analysis. Spectra were recorded at 313 and 403 K, coadding 500 scans at a resolution of $\pm 4.0\,cm^{-1}$. These spectra were collected in reflectance units and submitted to Kubelka–Munk transform.

Specific surface area was determined by the BET method from N_2 adsorption data at 77 K using a Belsorp 28SA (Bell). The samples were outgassed at 333 K for 6 h before measuring the nitrogen adsorption.

SEM and EPMA experiments were carried on a Jeol JXA-8900L WD/ED combined microanalyzer. The catalysts were initially fixed on a carbon tape and then coated with carbon by conventional sputtering techniques. The employed accelerating voltage was 20 kV and current ca. 3×10^{-8} A for EPMA and ca. 1×10^{-10} A for SEM.

3. Results and discussion

Silica was modified with MAO toluene solutions corresponding to 0.5–20.0 wt.% Al/SiO_2. The Al content was determined by ICP-OES after acid digestion. The results are shown in Table 1. For comparative reasons, data from the commercial MAO-modified silica were also included.

According to the results presented in Table 1, the Al detected amount increases up to sample corresponding to 10.0 wt.%, and then decreases, and finally increases again, presenting the sample 20 wt.% roughly the same Al amount as that corresponding to 10 wt.%. The Al density for values higher than the saturation level (higher than 10.0 wt.% Al/SiO_2) remains about 10–13 Al nm^{-2} values.

Inspite of using the impregnation method, for initial Al contents higher than 10.0 wt.%, the final metal content does not increase linearly. Probably part of the aluminum moieties (specially that corresponding to TMA species) might be removed during the drying step.

It is worth mentioning that silicas treated at 723 K under vacuum present OH density close to 1.5 OH nm^{-2} [12]. In such case, for loadings below the

Table 1
Aluminum concentration determined by ICP-OES

Sample	Al content	
	[Al][a]	Al nm^{-2}
0.0	0.00	0.0
0.5	0.37	1.1
2.0	1.02	3.1
4.0	1.10	3.3
10.0	4.22	12.7
15.0	3.37	10.2
20.0	4.30	13.1
24.4	8.43	25.4

[a] Expressed in mmol Al g^{-1} catalyst.

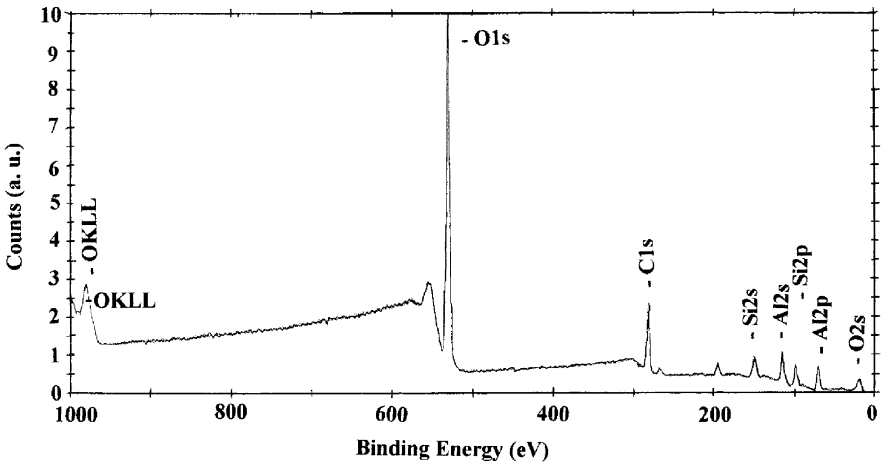

Fig. 1. XPS survey spectrum of MAO/SiO_2 (4.0 wt.% Al/SiO_2).

surface saturation, there is roughly 1 or 2 Al atoms for each isolated silanol group. Nevertheless, such ratio is much higher for higher Al loadings, indicating that most of the Al atoms are not directly bound to silica surface.

The systems were also evaluated by XPS to identify the surface composition and nature of the surface species. XPS has been used to determine surface coverage and binding energies of silica surfaces treated with silanes [13]. A representative survey spectrum of the MAO-supported silica is shown in Fig. 1. The constituent atoms of the catalysts (Si, O, C and Al) were observed to exist on the XPS measurable surface, approximately 5 nm in sampling depth.

The atomic surface composition was also evaluated by XPS. For comparative reasons data concerning the commercial MAO-modified silica were also included (Table 2).

As we can see in Table 2, the increase in MAO concentration in the impregnation solution leads to an increase in the amount of surface aluminum up to 62.5%, then decreases to 49.5% and then increases reaching 65.2% at 20.0 wt.% Al/SiO_2 system. In order to evaluate the depth profile, the analysis of the 0.5 and 10.0 wt.% Al/SiO_2 systems were evaluated at takeoff angles between 75° and 25°. Since the XPS analysis provide the atomic percentage which might change in function of the X-ray depth, we expressed the surface composition in terms of Al/Zr ratio instead of wt.% Al/SiO_2 or wt.% Zr/SiO_2.

As we can see in Fig. 2, in the case of low Al coverage, a much higher Al/Si ratio is observed at the more surface glancing at $\alpha = 20°$ than at $\alpha = 75°$, indicating that the grafted layer is restricted to the outermost surface of silica substrate. In the case of the 10.0 wt.% Al/SiO_2, the Al/Si ratio variation is much lower, indicating that a external surface layer is more homogenous for the same depth.

Fig. 3 shows the Si 2p core-level spectra of some MAO-supported silicas. The Si 2p spectrum of silica surface contains a major peak component at the binding energy (BE) of 103.3 eV, associated to silica atoms in the bulk. The lower BE component (101.1 eV) can be attributed to the outermost layer of Si atoms. The latter corresponds to ca. 20% of total area. The impregnation of 0.5 wt.% Al/SiO_2 inspite of not causing

Table 2
Atomic surface composition determined by XPS

Sample	Element content (at. wt.%)	
	Al	Al/Si
0.0	0.0	0.0
0.5	23.4	0.3
2.0	26.9	0.4
4.0	40.2	0.7
10.0	62.5	1.6
15.0	49.6	1.8
20.0	65.2	8.9
24.4	89.9	9.0

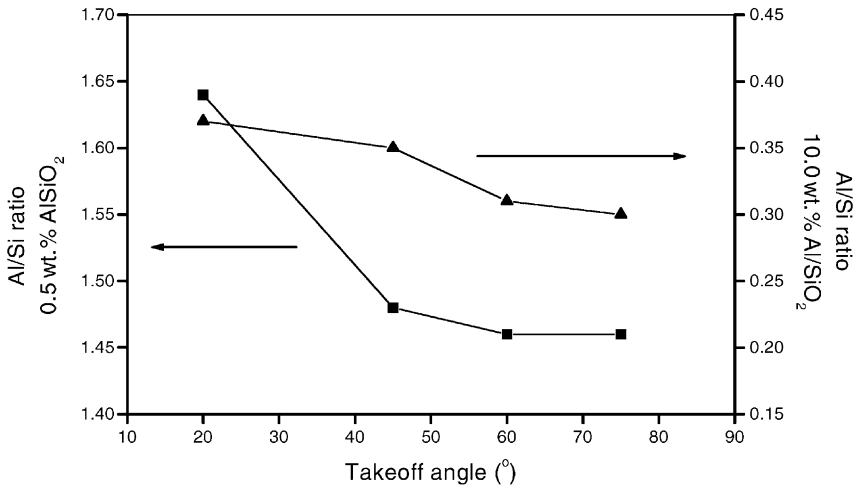

Fig. 2. Relationship between the Al/Zr ratio and the takeoff angle.

any substantial BE shift, leads to an increase in the FWHM value, indicating a more heterogeneous nature on the outermost surface species. In the case of 20.0 wt.% Al/SiO_2 (spectrum (c) in Fig. 3) we observe an even higher signal broadness, besides a shift to higher BE in the case of 0.5 wt.% Al/SiO_2.

Table 3 shows the Si deconvolution parameters of the different MAO-supported silicas. Concerning the low BE component, there is a tendency in increasing the BE as the amount of Al increases, suggesting a reduction in the electron density in the silica surface atoms for concentrations up to 10.0 wt.%. Taking into account the FWHM values, there is also an increase in the surface heterogeneity. This is a manifestation of the greater diversity of local chemical environments that the surface silicon experiences upon MAO impregnation.

The Al 2p core-level spectra of some supported systems are shown in Fig. 4. In the case of 0.5 wt.% Al/SiO_2 a broad signal (FWHM = 3.0) can be observed at 74.0 eV. As we enhance the Al content (4.0 wt.% Al/SiO_2, spectrum (b)) the FWHM becomes larger, suggesting an heterogeneity in the surface composition. For values above the surface saturation (10.0 wt.% Al/SiO_2), the Al 2p spectrum can only be curve-fitted with two peak components corresponding to two surface species, the lower BE component indicating an electron richer species.

The deconvolution of Al parameters for the supported systems are presented in Table 4. For the systems below the saturation level, only one species is detected, showing an increase in BE with the surface coverage going from 0.5 to 4.0 wt.% Al/SiO_2. The increase in FWHM values supports a greater variety of surface states. On the other hand, for Al contents higher than the saturation amount, two signals are

Table 3
Si core-level XPS data of the MAO-supported systems

Al/SiO_2 (wt.%)	BE[a] (eV)	Relative elemental abundance (%)	FWHM[b] (eV)
0.0	103.3	80	2.4
	101.2	20	2.1
0.5	103.3	81	2.7
	101.2	19	2.5
2.0	103.4	69	2.9
	101.3	31	3.1
4.0	103.3	84	3.4
	101.7	16	3.2
10.0	103.2	82	3.2
	101.8	18	3.4
15.0	103.2	88	2.8
	100.8	12	2.6
20.0	103.3	75	2.5
	101.4	25	2.4
24.4	103.3	80	2.7
	101.5	20	2.9

[a] Reference: Si 2p from SiO_2 (103.3 eV).
[b] Full width at half maximum intensity.

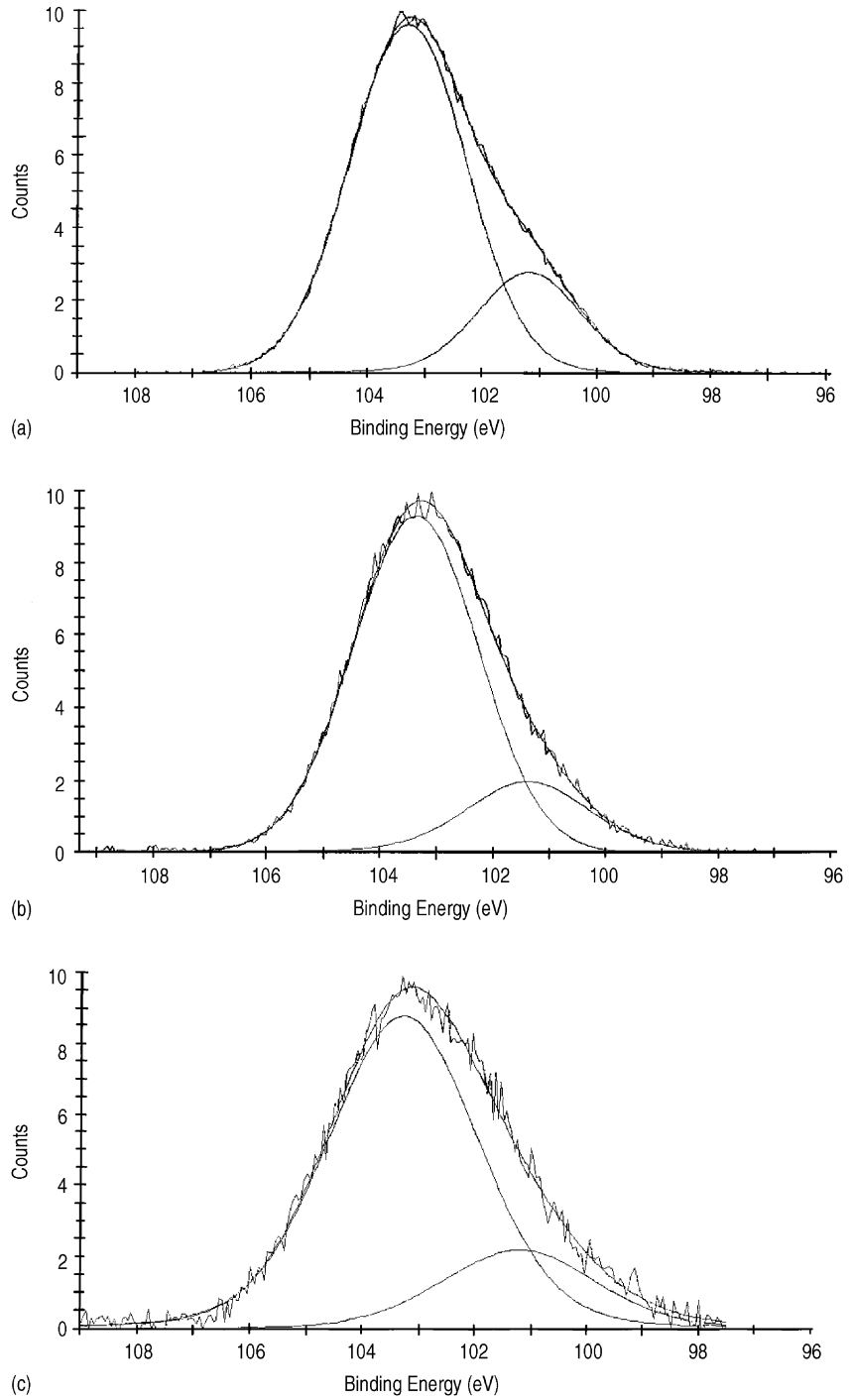

Fig. 3. Si core-level XPS spectral curve fitting. The small inserted peaks are the curve fit components, which are summed to obtain the smooth drawn line. The line with a visible noise component is the experimental raw data: (a) SiO_2; (b) 0.5 wt.% Al/SiO_2; (c) 20.0 wt.% Al/SiO_2.

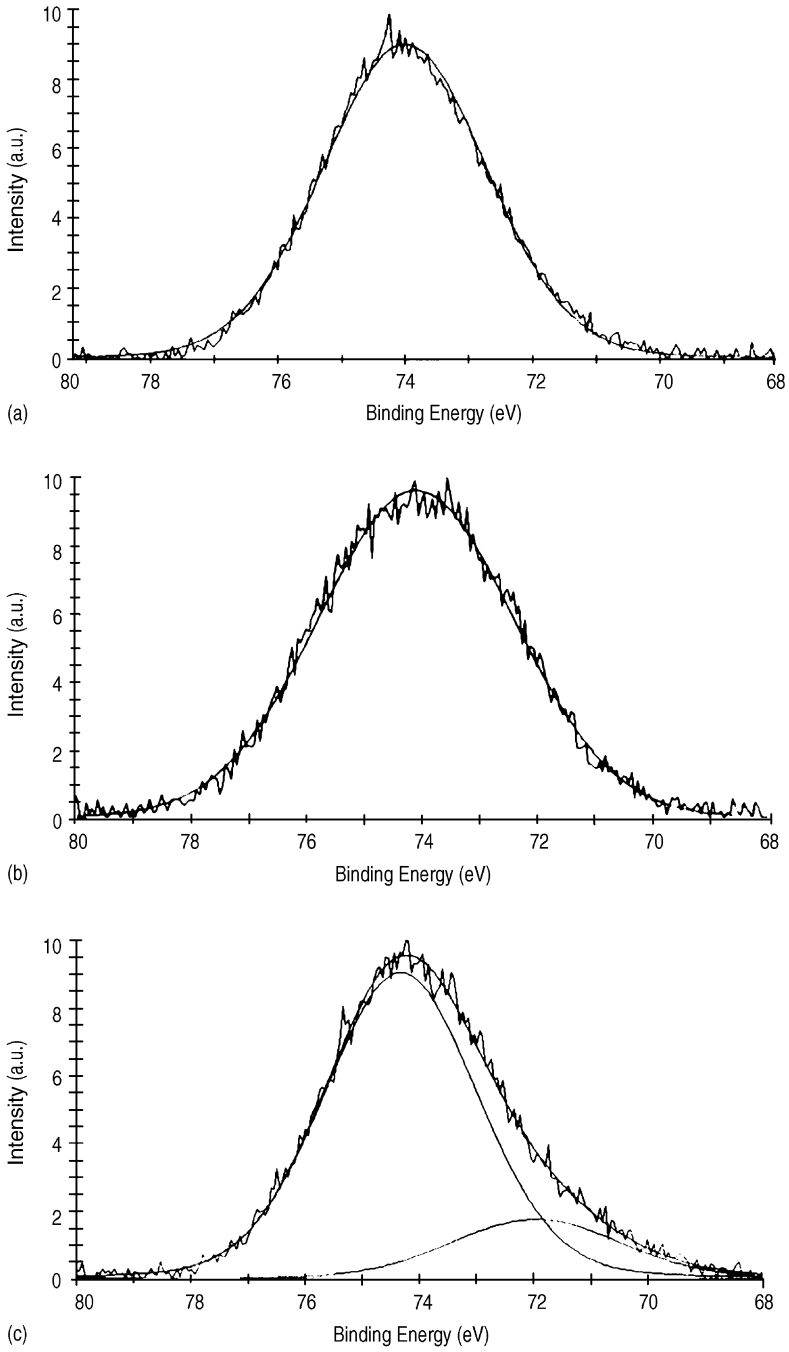

Fig. 4. Al core-level XPS spectral curve fitting. The small inserted peaks are the curve fit components, which are summed to obtain the smooth drawn line. The line with a visible noise component is the experimental raw data: (a) 0.5 wt.% Al/SiO_2; (b) 4.0 wt.% Al/SiO_2; (c) 10.0 wt.% Al/SiO_2.

Table 4
Al core-level XPS data of the MAO-supported systems

Al/SiO_2 (wt.%)	BE[a] (eV)	Relative elemental abundance (%)	FWHM[b] (eV)
0.0	–	–	–
0.5	74.0	100	3.0
2.0	74.3	100	3.1
4.0	74.6	100	4.1
10.0	74.3	86	3.2
	71.8	14	3.2
15.0	74.5	83	2.5
	72.6	17	2.2
20.0	74.5	84	2.6
	72.5	16	2.0
24.4	74.6	88	2.3
	72.7	12	2.0

[a] Reference: Si 2p from SiO_2 (103.3 eV).
[b] Full width at half maximum intensity.

Table 5
Al core-level XPS data of the MAO-supported systems at different takeoff angles

Takeoff angle	BE (eV)	Relative elemental abundance (%)	FWHM (eV)
Al/SiO_2 (0.5 wt.%)			
75	74.0	100	3.0
60	74.3	72	3.0
	72.2	28	3.7
45	74.1	81	2.7
	71.9	19	3.2
20	74.2	79	2.9
	72.3	21	2.7
Al/SiO_2 (10.0 wt.%)			
75	74.3	86	3.2
	71.6	14	3.2
60	73.8	83	2.8
	71.7	17	2.3
45	74.6	80	3.2
	71.3	20	4.1
20	74.4	86	3.0
	72.2	14	2.9

detected, corresponding to two surface species. The major peak component corresponds to ca. 85% of the signal and takes place in BE values close to those of the low Al content. The lower BE component shifts remains closer to 72.5 eV for MAO-modified higher than 10.0 wt.%, indicating a reduction in electron density in such systems, in comparison to that observed in the case of 10.0 wt.% Al/SiO_2 system.

The presence of two signals for higher Al contents can be a consequence from the existence of very exposed Al species in the outermost surface layer. Table 5 shows the deconvolution parameters for Al, measured at different takeoff angles. For 0.5 wt.% Al/SiO_2, as already mentioned, only one signal was detected. Nevertheless, for the same sample, as the takeoff angles decreases, a second peak is detected at the lower BE side, corresponding to ca. 20–28% of total area, suggesting that even at low Al coverage, there is Al atoms which are more exposed. This fact can in part attributed to the oligomeric structure of MAO, which might be kept during the surface reaction. Similar behavior was observed in the case of the two components of the 10.0 wt.% Al/SiO_2.

The systems were further analyzed by UV–VIS measurements. The 200–560 nm region of the UV spectrum of the 0.5 wt.% Al/SiO_2 supported system is shown in Fig. 5a. An intense band is observed at 271 nm with a shoulder at 289 nm, which is much closer to that reported in the case of MAO in benzene solution (286 nm). The transition in the near UV–VIS region can only be attributed to the nonbonding electrons of bridging oxygens, which are available for the electronic transition.

As we increase the MAO content on silica surface (10 wt.% Al/SiO_2), two bands are distinguished: 269 and 286 nm, indicating an increase in the amount of the species responsible for the absorption at 286 nm. Higher Al amount (20 wt.% Al/SiO_2) shows a large band centered at 299 nm. This bathochromic shift with the Al content increase may be explained in terms of a strong interaction of the nonbonding oxygens electrons with neighboring Al atoms [14]. In other words, as expected, increasing the Al amount other Al species are observed, which are more available to an oxygen to aluminum $p\pi$–$d\pi$ dative bond. Such species corresponds to the low BE signal detected by XPS measurements for higher surface Al content.

The surface species were also evaluated by DRIFTS. Fig. 6 shows the infrared spectra for silica at different MAO contents. Table 6 presents the probable assignments based on the literature [15]. For the lower

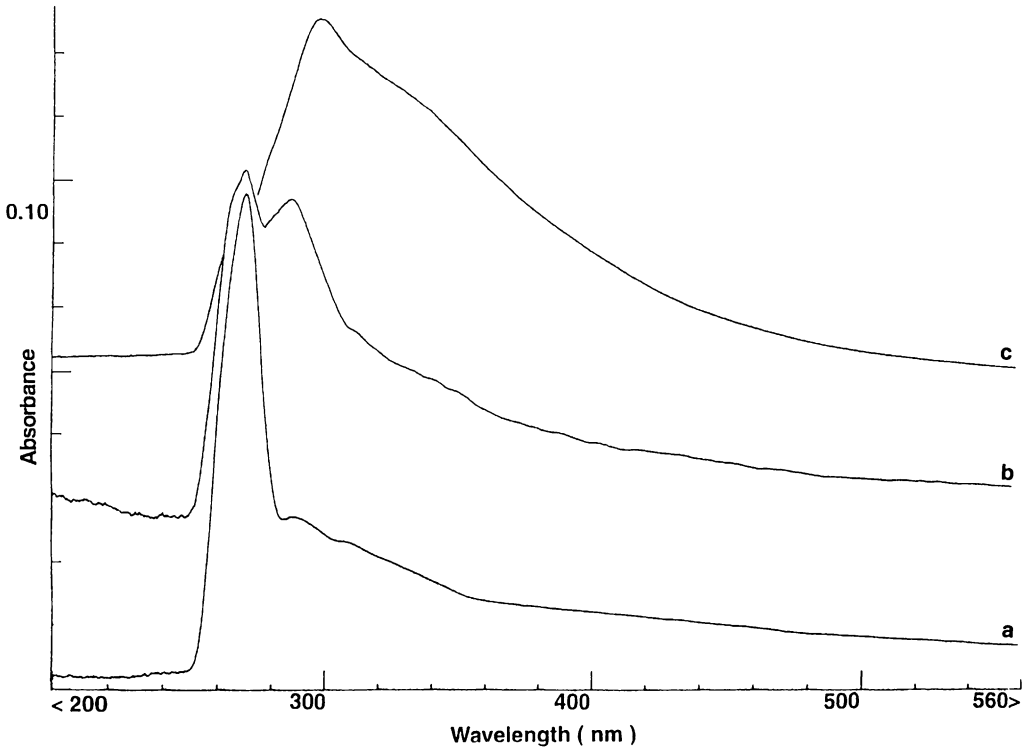

Fig. 5. UV–VIS spectra of MAO-modified silicas at room temperature: (a) 0.5 wt.% Al/SiO_2; (b) 10.0 wt.% Al/SiO_2; (c) 20.0 wt.% Al/SiO_2.

metal content (0.5–4.0 wt.% Al/SiO_2) we can observe the presence of isolated silanol groups (3746 cm^{-1}). Such groups disappear for MAO content higher than 10.0 wt.% Al/SiO_2 in agreement with MAO adsorption on silica isotherm measurements [11].

The methyl groups from MAO can be observed in the bands situated between 3000 and 2800 cm^{-1}. Terminal CH_3 groups are expected to present ν_a and ν_s between 3050–2810 and 2950–2750 cm^{-1}, respectively.

Table 6
IR bands assignments to MAO-modified silicas

Band wavenumber (cm^{-1})	Vibrational mode
3746 ± 1	Isolated ν(OH)
3650 ± 6	Intraglobular ν(OH)
3395 ± 5	–
3240 ± 2	–
2960 ± 2	ν(Si–CH_3)
2902 ± 2	ν(Si or Al–CH_3)
2840 ± 2	ν((O)–CH_3)

Such groups are extremely sensitive to the existence of intermolecular interactions, and consequently by changes in symmetry.

In the case of 2.0 wt.% Al/SiO_2, three bands are detected: 2962, 2908 and 2840 cm^{-1}. The reactions between TMA and silanol groups are known for a long time and it is the basis of a well-established method for surface OH determination [16]. Such reactions are relatively complex generating surface species issued basically from the reaction of TMA with silanol or siloxane groups. These species are well studied and reported in the literature [17]. The resulting species give rise to absorption bands in the C–H region: 2940, 2900 and 2830 cm^{-1} for Al–CH_3; 2960 and 2900 cm^{-1}, for Si–CH_3. Thus, it seems that in the case of reaction between MAO and silica, Si–CH_3 species can also be generated (2960 cm^{-1}).

The shoulder at 2840 cm^{-1} increases in intensity as the MAO content increases. In the case of reaction between TMA and silica, the presence of a peak at 2860 cm^{-1} corresponds to one of the three CH

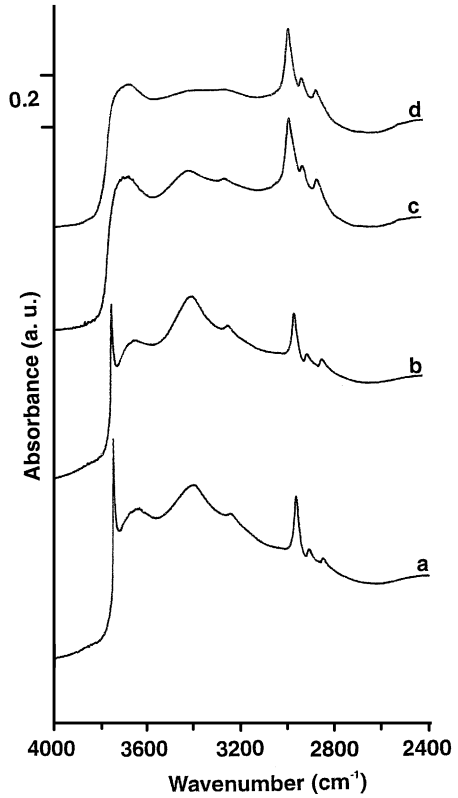

Fig. 6. DRIFTS spectra of MAO-modified silicas measured at 40 °C: (a) 0.5 wt.% Al/SiO_2; (b) 2.0 wt.% Al/SiO_2; (c) 10.0 wt.% Al/SiO_2; (d) 15.0 wt.% Al/SiO_2.

stretching peaks in the spectrum of methoxy groups, along with peaks at 3000 and 2960 cm^{-1}. Peaks at 2857 cm^{-1} were already observed in the immobilization of MAO on silica [18] and attributed to methoxy groups from MAO in analogy with the structure proposed by Atwood et al. [19].

Moreover, comparing spectrum (a)–(d), we can also see that in the C–H region the bands became broader, suggesting an increase in the heterogeneity in the nature of the surface species.

In the spectra of Fig. 6 we can also observe other three bands situated between 3650 and 3200 cm^{-1}. The band at ca. 3650 cm^{-1} is attributed to intraglobular OH groups retained inside the pores [20]. The relative intensities of the two other bands, 3395 and 3240 cm^{-1}, decrease as the number of isolated OH groups decreases (compare spectrum (a)–(d)). Therefore, it seems that such bands are resulting from OH

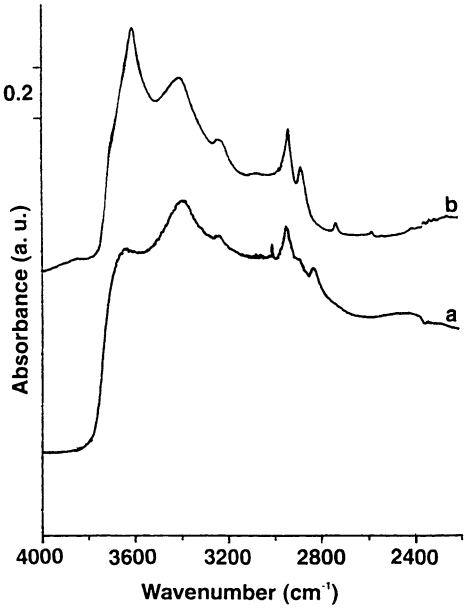

Fig. 7. DRIFTS spectra of modified silicas measured at 40 °C: (a) 20 wt.% Al/SiO_2 (MAO-modified silica); (b) 4.0 wt.% Al/SiO_2 (TMA-modified silica).

groups which are perturbed by the presence of MAO adsorption, probably by intramolecular interaction with oxygen atoms from MAO oligomers.

Fig. 7 shows the spectrum of the 20.0 wt.% Al/SiO_2 MAO-modified support. For comparative reasons, DRIFTS result for the 3.0 wt.% Al/SiO_2 TMA-modified support was also included (spectrum (b)). Comparing spectrum (a) of Fig. 7 to (d) of Fig. 6, we can observe that the intensity of $\nu_{(CH)}$ bands are lower than those corresponding to 15 wt.% Al/SiO_2. Such results are in agreement with those obtained by ICP-OES and XPS. The corresponding spectrum in the case of TMA presents the bands at 3604 cm^{-1} (intraglobular OH) and the two other bands at 3398 and 3235 cm^{-1}. The band corresponding to isolated OH groups is absent, suggesting that such groups were totally consumed at such Al loading. Such results are also in agreement with previously TMA adsorption isotherm determination which evidenced silica surface saturation at ca. 3.0 wt.% Al/SiO_2 [11].

In the $\nu_{(CH)}$ region, two signals were observed at 2927 and 2879 cm^{-1}. Comparing both spectra in Fig. 7, it seems that the support modified with 20 wt.% Al/SiO_2 is constituted of a mixture of species issued

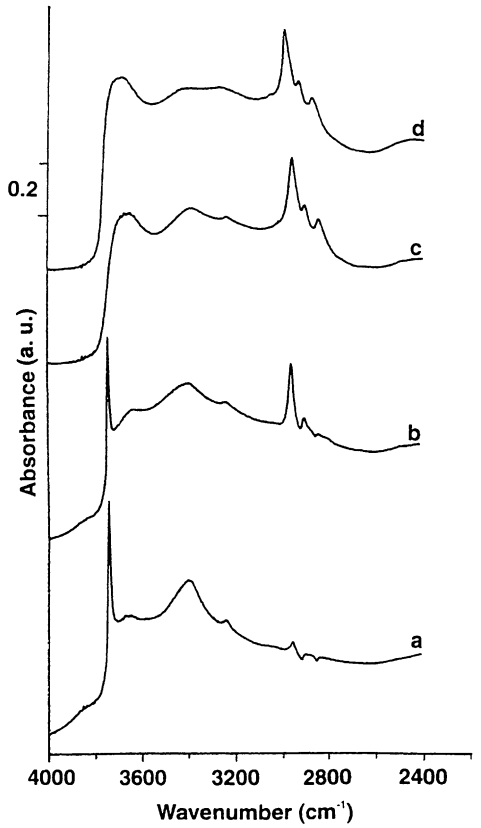

Fig. 8. DRIFTS spectra of MAO-modified silicas after thermal treatment: (a) 4.0 wt.% Al/SiO_2 (313 K); (b) 4.0 wt.% Al/SiO_2 (403 K); (c) 10.0 wt.% Al/SiO_2 (313 K); (d) 10.0 wt.% Al/SiO_2 (403 K).

from MAO and TMA surface adsorption. Inspite of the high concentration of TMA and its lower steric hindrance in comparison to MAO oligomers, part of the generated surface species are also issued from MAO adsorption.

The thermal stability of MAO-modified silicas were evaluated by submitting the supports to in situ thermal treatment for 1 h at 353 and 403 K, which corresponds to temperature usually employed for metallocene immobilization or polymerization [21]. Fig. 8 illustrates two modified supports (4.0 and 10.0 wt.% Al/SiO_2) submitted to two thermal treatments (313 and 403 K). In the case of 4.0 wt.% Al/SiO_2 support, we observe a reduction in the intensity of the bands corresponding to isolated OH and methyl groups. It seems that the presence isolated silanol groups can promote the decomposition of surface methyl groups, probably by evolving of methane.

Table 7
Textural properties of MAO-modified silicas

Al/SiO_2 (sample wt.%)	A_p ($m^2\,g^{-1}$)	V_p ($mm^3\,g^{-1}$)	R_p (nm)
0.0	256	56	11
0.5	259	59	12
2.0	250	57	15
4.0	245	55	18
10.0	210	48	14
15.0	261	60	12
20.0	252	58	12

In the case of 10.0 wt.% Al/SiO_2, no significative modification takes place, probably due to the absence of free silanol groups. Nevertheless, a reduction in the intensities of the bands located at 3395 and 3240 cm^{-1} is observed.

It is worth mentioning that during metallocene immobilization, part of such residual silanol groups might be consumed, reducing therefore such thermal instability in the case of MAO content lower than 10.0 wt.% Al/SiO_2.

Recently, Lewis acid sites on TMA- and MAO-modified silica were measured by CO adsorption at 77 K using transmission infrared spectroscopy [22,23]. The use of CO as probe molecule in our samples using DRIFTS measurements did not provide evidences of chemical interaction at 298 K. The CO generated species observed between 2300 and 2100 cm^{-1} were promptly removed by vacuum.

Grafting organometallics on supports can influence the final support texture. For instance, microporosity developing was observed in the case of grafting silicon ethoxide on aluminas [24]. In order to evaluate the effect of increasing MAO content on silica textural properties (surface area, A_p, pore volume, V_p and mean pore radius, R_p), we performed nitrogen adsorption using the BET method.

Table 7 reports data concerning textural properties of silica modified with different Al contents. According to these data, no significative modification could be observed in silica texture after MAO immobilization. In other words, it seems that MAO does not occupy part of the pore volume of the silica support (which would lead to a decrease of A_p, V_p or R_p). Neither, MAO oligomers on the surface develop their

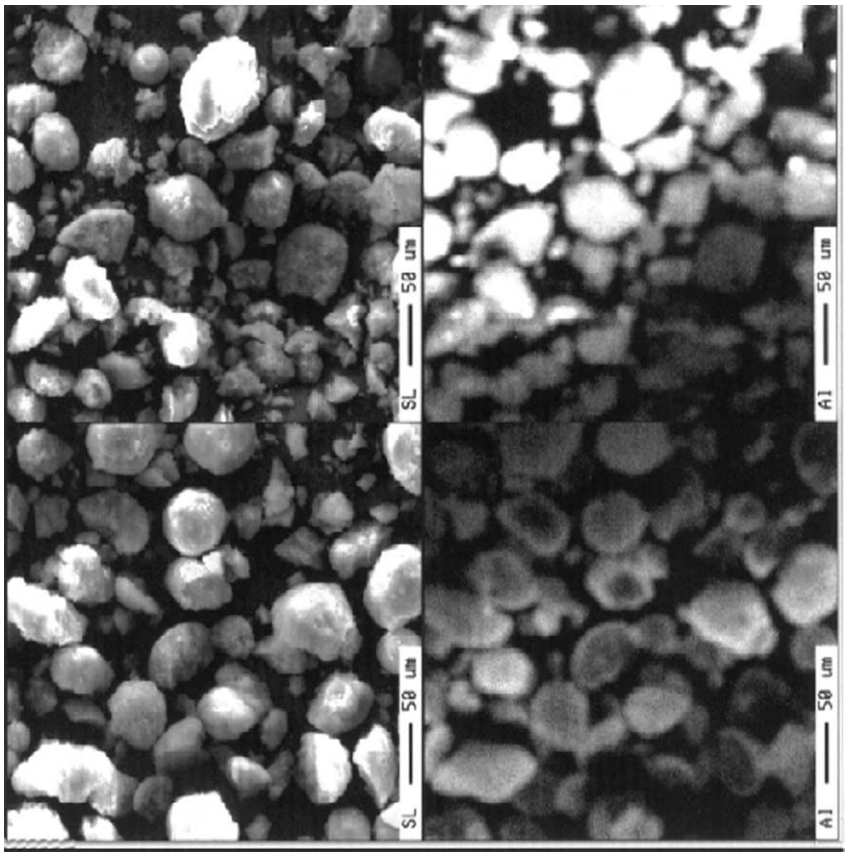

Fig. 9. SEM photographs of MAO-modified silica (left) and element distribution map of Al in the resulting solids (right): 4.0 wt.% Al/SiO_2 (bottom); 15.0 wt.% Al/SiO_2 (top).

own porosity, which would cause an increase in the surface area.

The morphology of the supports was evaluated by SEM. Fig. 9 (left) shows two micrographs of MAO-modified silica, below and above the saturation level. In the case of 4.0% Al/SiO_2 system, the initial silica morphology is roughly kept identical. Nevertheless, for higher initial Al concentrations (15.0 wt.% Al/SiO_2), abundant irregular fine particles can be observed. The spatial distribution of Al on silica can be evaluated by EPMA, by detecting their characteristic X-ray emission. The resulting Al distribution maps on the silica particle are shown in Fig. 9 (right). Low metal content corresponds to the darker region, while higher metal content, to the brighter one. According to EPMA analysis, we can observe that the fine particles are constituted by practically pure aluminum. Thus, it is very likely that such debris come from layers of pure MAO covering the silica particles that detach from the rest of the particle. Similar results were reported for commercially high loaded silica (23 wt.% Al/SiO_2) and detected by EDX analysis [25]. It seems that high level of MAO coating might produce supports which are more prone to leaching during zirconocene grafting or even during polymerization.

4. Conclusion

The amount of commercial MAO for the modification of silica seems to influence the nature of surface species. Different species are generated depending on the alumina concentration in the initial solution. Surface saturation seems to take place at about 10.0 wt.%

Al/SiO_2. It is worth noting that TMA present in commercial MAO seems to play an important role on the final immobilized Al content as well as on the nature of the surface species. High contents of MAO might coat the silica surface which layers seems to be more prone to detach from the rest of the particle.

As Barron [7] stated the difficulties that must be overcome in characterizing alkylaluminoxanes in solution will only be amplified in the solid state. Further studies have been carried on the effect of such MAO-modified silicas as supports for immobilizing metallocenes on catalyst activity and on polymer properties.

Acknowledgements

Financial support for Prof. J.H.Z. dos Santos has been provided by the Japan Society for Promotion of Science (JSPS).

References

[1] J. Scheirs, W. Kaminsky (Eds.), Metallocene-based Polyolefins, Wiley, West Sussex, 2000.
[2] (a) G.G. Hlatky, Chem. Rev. 100 (2000) 1347;
(b) H.T. Ban, T. Arai, C.-H. Ahn, T. Uozumi, K. Soga, Curr. Trends Polym. Sci. 4 (1999) 47;
(c) M.R. Ribeiro, A. Deffieux, M.F. Portela, Ind. Eng. Chem. Res. 36 (1997) 1224.
[3] J.H.Z. dos Santos, H.T. Ban, T. Teranishi, T. Uozumi, T. Sano, K. Soga, J. Mol. Catal. A Chem. 158 (2000) 541.
[4] P.J. Tait, R. Ediati, in: W. Kaminsky (Ed.), Metalorganic Catalysts for Synthesis and Polymerization, Springer, Heidelberg, 1999, p. 307.
[5] E.Y.-X. Chen, T.J. Marks, Chem. Rev. 100 (2000) 1391.
[6] M.R. Mason, J.M. Smith, S.G. Bott, A.R. Barron, J. Am. Chem. Soc. 115 (1993) 4971.
[7] A.R. Barron, in: J. Scheirs, W. Kaminsky (Eds.), Metallocene-based Polyolefins, Wiley, West Sussex, 2000.
[8] (a) S. Psynkiewicz, Polyhedron 9 (1990) 429;
(b) H. Sinn, J. Bliemeister, D. Clausnitzer, L. Tikwe, H. Winter, O. Zarncke, in: W. Kaminsky, H. Sinn (Eds.), Transition Metals and Organometallics as Catalysts for Olefin Polymerization, Springer, New York, 1988, p. 257;
(c) I. Tritto, C. Mealares, M.C. Sacchi, P. Locatelli, Macromol. Chem. Phys. 198 (1997) 3963.
[9] J.L. Eilertsen, E. Rytter, M. Ystenes, Vibrat. Spectrosc. 24 (2000) 257.
[10] V.N. Panchenko, V.A. Zakharov, I.G. Danilova, E.A. Paukshtis, I.I. Zakharov, V.G. Goncharov, A.P. Suknev, J. Mol. Catal. A 174 (2001) 107.
[11] J.H.Z. dos Santos, S. Dorneles, F.C. Stedile, J. Dupont, M.C. Forte, I.J.R. Baumvol, Macromol. Chem. Phys. 198 (1997) 3529.
[12] S. Ogasawara, Shokubai 18 (1976) 124.
[13] (a) M.L. Miller, R.W. Linton, S.G. Bush, J.W. Jorgenson, Anal. Chem. 56 (1984) 2204;
(b) M.L. Miller, R.W. Linton, Anal. Chem. 57 (1985) 2314;
(c) K.M.R. Kallury, P.M. Macdonald, M. Thompson, Langmuir 10 (1994) 492.
[14] E. Gianetti, G.M. Nicoletti, R. Mazzocchi, J. Polym. Sci., Polym. Chem. 23 (1985) 2117.
[15] (a) N.B. Colthup, L.H. Daly, S.E. Wiberley, Introduction to Infrared and Raman Spectroscopy, 2nd Edition, Academic Press, New York, 1975, p. 277;
(b) B.A. Morow, Stud. Surf. Sci. Catal. 57A (1990) A161.
[16] (a) J.C.W. Chien, J. Am. Chem. Soc. 93 (1971) 4675;
(b) M.J.D. Low, A.G. Severdia, J. Low, J. Catal. 69 (1981) 384;
(c) B.A. Morrow, A.H. Hardiei, J. Phys. Chem. 83 (1979) 3135.
[17] E.F. Vansant, P. Van Der Voort, K.C. Vrancken, Characterization and Chemical Modification of the silica surface, Elsevier, Amsterdam, 1995, pp. 366–367.
[18] J.H.Z. dos Santos, C. Krug, M.B. da Rosa, F.C. Stedile, J. Dupont, M.C. Forte, J. Mol. Catal. A 139 (1999) 199.
[19] J.L. Atwood, D.C. Hrncir, R.D. Priester, R.D. Rogers, Organometallics 2 (1983) 985.
[20] E.F. Vansant, P. Van Der Voort, K.C. Vrancken, Characterization and Chemical Modification of the Silica Surface, Elsevier, Amsterdam, 1995, p. 66.
[21] J.H.Z. dos Santos, M.B. da Rosa, C. Krug, F.C. Stedile, M.C. Haag, J. Dupont, M.C. Forte, J. Polym. Sci., Part A Polym. Chem. 37 (1999) 1987.
[22] V.A. Zakharov, V.N. Panchenko, N.V. Semikolenova, I.G. Danilova, E.A. Paukshtis, Polym. Bull. 43 (1999) 87.
[23] V.N. Panchenko, N.V. Semikolenova, I.G. Danilova, E.A. Paukshtis, V.A. Zakharov, J. Mol. Catal. A Chem. 142 (1999) 27.
[24] P. Sarrazin, S. Kasztelan, N. Zanier-Szydlowski, J.P. Bornelle, J. Grimblot, J. Phys. Chem. 97 (1993) 5947.
[25] A. Muñoz-Escalona, L. Méndez, J. Sancho, P. Lafuente, B. Peña, W. Michels, G. Hidalgo, M.F. Martinez-Nuñez, in: W. Kaminsky (Ed.), Metalorganic Catalysts for Synthesis and Polymerization, Springer, Heidelberg, 1999, p. 381.